PHYSICS AND CHEMISTRY OF SOLID STATE
V. 23, No. 2 (2022) pp. 285-292
Section: Physics

DOI: 10.15330/pcss.23.2.285-292

Vasyl Stefanyk Precarpathian National University

ФІЗИКА І ХІМІЯ ТВЕРДОГО ТІЛА
Т. 23, № 2 (2022) С. 285-292

Фізико-математичні науки

PACS numbers: 43.35.Cg; 62.20.Dc; 63.20.Kr; 65.80.+n

ISSN 1729-4428

Pramod K. Yadawa[1*], Navin Chaurasiya[1,2], Sachin Rai[1] and Aadesh K. Prajapati[1]

Investigation of the Effect of Temperature on Ultrasonic, Mechanical and Thermal Properties in Single Silver Nanowire

[1]*Department of Physics, Prof. Rajendra Singh (RajjuBhaiya) Institute of Physical Sciences for Study and Research, V. B. S. Purvanchal University, Jaunpur, India- 222003, pkyadawa@gmail.com*
[2]*Department of Mechanical Engineering, UNSIET, V. B. S. Purvanchal University, Jaunpur, India- 222003*

The present paper reports the elastic, mechanical and thermophysical properties of silver nanowire (Ag NW) using ultrasonic techniques at temperature dependent. Higher order elastic constants are calculated using Coulomb and Born-Mayer potential up to second nearest neighbour. To compute mechanical parameters such as young modulus, bulk modulus, shear modulus tetragonal modulus, Poisson's ratio, fracture to toughness ratio and Zener anisotropy factor for finding imminent performance of the single silver nanowire at temperature dependent using second order elastic constants. The Ag NW is found to be brittle in nature at room temperature. Finally, we have evaluated the ultrasonic velocities, ultrasonic attenuation due to phonon–phonon interaction and thermoelastic relaxation for longitudinal wave and shear waves along <100>, <110> and <111> crystallographic directions in the temperature range 100 - 300 K of silver nanowire using the higher order elastic constants. The attained results are discussed in correlation with available outcomes on these properties for the silver nanowire.

Key words: silver nanowire, elastic properties, thermal properties, ultrasonic properties.

Received 6 October 2021; Accepted 18 May 2022.

Introduction

Silver nanowire was fascinated significant attention due to its outstanding mechanical, thermal, optoelectronic properties [1, 2] and excellent applications like solar cells, optoelectronic energy converters, thermal interface materials, flexible touch screen, transparent electrodes etc. [3-5]. The mechanical and thermal properties of a specific Ag NW are critical and essential but they were hardly reported for the optimization and design of these applications. Stojanovic et al. [6] have evaluated the thermal conductivity of aluminium NW arrays instead of a single nanowire. For metallic nanostructure materials, when size of the system is lesser than the bulk electron mean free path, the surface and grain boundary become significant scattering sources which limit the electron mean free path and then decrease the electrical and thermal conductivities. Recently Chang et al. have established the interaction between the behaviour of silver single-crystalline NWs and atomic arrangement with face-centered cubic (fcc) structure. It follows the compact dimensional scale of the NW increases the yield strength [7]. Silver nanowires (Ag NW) used in this work have prepared by Cheng et al. [8]. Ag NW have purchased from Sigma-aldrich and supplied as suspensions in isopropyl alcohol (IPA) with a concentration of 0.5%. The silver nanowires remained on the gel film after IPA evaporated. In this process, the dispersion has diluted to a degree that single silver nanowires stayed on the gel film without contact with the surrounding ones. X-ray diffraction have used to analyze the fcc structure of the Ag NW. The electrical resistivity of Ag NW is five times larger than bulk silver at room temperature. This is due to the combined effect of various structural and phonon scatterings. For bulk silver, the phonon-electron scattering dominates at room temperature. But for the silver nanowire, both the phonon scattering and structural scatterings contribute to the large electrical resistivity. Also, the thermal conductivity of the silver nanowire decreased with decreasing temperature while that of the bulk silver increased.

At the nanoscale, the mechanical properties of the

materials are changed from macroscopic scale due to the increasing ratio of the surface to the volume. The surface effect can be substantial for the nano structural compounds with a large ratio of the surface area to the bulk [9]. Cuenot et al. [10] analyzed both experimentally and theoretically the surface effect on the elastic moduli of silver and lead NWs. Bulk silver shows that the maximum thermal and electrical conductivity between the metals. Silver nanowires are predictable to be good conductors in nanoscale electronic devices [11]. Silver NWs hold auspicious potential as elastic electrodes [12].

In the present investigation, the second order elastic constants (SOECs) and third order elastic constants (TOECs) of Ag NW have been investigated at temperature range 100 - 300 K using Coulomb and Born-Mayer potential. The calculated values of SOECs are useful to compute mechanical properties of this nanowire like Young's modulus, bulk modulus, shear modulus, tetragonal modulus, Zener anisotropy factor, Poisson's ratio and fracture to toughness ratio for Ag NW for forthcoming performance. Also, find the temperature dependent ultrasonic velocities, ultrasonic Grüneisen parameters and ultrasonic attenuations along <100>, <110> and <111> crystallographic directions using SOECs and TOECs. The obtained results are discussed in correlation through known physical properties of nanowires.

I. Theory

Using Born Mayer Potential approaches, temperature-dependent second-order and third-order non-linear elastic constant for fcc structured Ag nanowires have been calculated. Firstly, the theoretical invention for the calculation of second order elastic constants (SOECs) and third order elastic constants (TOECs) have developed by Brugger [13] and then consecutively established by Ghate [14] and Mori and Hiki [15]. The SOECs and TOECs are found by adding the static and vibrational contribution at particular temperature to the elastic constants as follows:

$$C_{IJ} = C^0_{IJ} + C^{Vib}_{IJ}, \qquad C_{IJK} = C^0_{IJK} + C^{Vib}_{IJK}, \tag{1}$$

here C^0_{IJ} and C^0_{IJK} are strain derivatives and C^{Vib}_{IJ} and C^{Vib}_{IJK} are strain derivatives of $F^{vib.}$, and signifies the static and vibrational elastic constants respectively. The extended expressions of SOECs and TOECs for static and vibrational terms as given as follows:

$$\begin{aligned}
C^0_{11} &= \frac{3e^2}{2r_0^4}S_5^{(2)} + \frac{1}{br_0}\left(\frac{1}{r_0}+\frac{1}{b}\right)\varphi(r_0) + \frac{2}{br_0}\left(\frac{\sqrt{2}}{2r_0}+\frac{1}{b}\right)\varphi(\sqrt{2}r_0),\\
C^0_{12} &= C^0_{44} = \frac{3e^2}{2r_0^4}S_5^{(1,1)} + \frac{1}{br_0}\left(\frac{\sqrt{2}}{2r_0}+\frac{1}{b}\right)\varphi(\sqrt{2}r_0),\\
C^0_{111} &= -\frac{15e^2}{2r_0^4}S_7^{(3)} - \frac{1}{b}\left(\frac{3}{r_0^2}+\frac{3}{br_0}+\frac{1}{b^2}\right)\varphi(r_0) - \frac{1}{2b}\left(\frac{3\sqrt{2}}{r_0^2}+\frac{6}{br_0}+\frac{2\sqrt{2}}{b^2}\right)\varphi(\sqrt{2}r_0),\\
C^0_{112} &= C^0_{166} = -\frac{15e^2}{2r_0^4}S_7^{(2,1)} - \frac{1}{4b}\left(\frac{3\sqrt{2}}{r_0^2}+\frac{6}{br_0}+\frac{2\sqrt{2}}{b^2}\right)\varphi\left(\sqrt{2}r_0\right),\\
C^0_{123} &= C^0_{144} = C^0_{456} = -\frac{15e^2}{2r_0^4}S_7^{(1,1,1)}
\end{aligned} \tag{2}$$

here b and r_0 represent the hardness parameter and the short-range parameter. Also $\phi(r_0)$ shows the Born-Mayer inter-ionic potential approaches given by $\phi(r_0) = A\exp(-r_0/b)$ and $\phi(\sqrt{2}r_0) = A\exp(-\sqrt{2}r_0/b)$

Strength parameter 'A' is given by: $A= -3b(e^2/r_0^2)[6\exp(-r_0/b)+12\sqrt{2}\exp(-r_0\sqrt{2}/b)]^{-1}$.

The vibrational term is shown by following expressions:

$$\begin{aligned}
C^{Vib}_{12} &= f^{(1,1)}G_1^2 + f^{(2)}G_{1,1}\\
C^{Vib}_{44} &= f^{(2)}G_{1,1}\\
C^{Vib}_{111} &= f^{(1,1,1)}G_1^3 + 3f^{(2,1)}G_2G_1 + f^{(3)}G_3\\
C^{Vib}_{112} &= f^{(1,1,1)}G_1^3 + f^{(2,1)}G_1(2G_{1,1}+G_2) + f^{(3)}G_{2,1}\\
C^{Vib}_{123} &= f^{(1,1,1)}G_1^3 + 3f^{(2,1)}G_1G_{1,1} + f^{(3)}G_{1,1,1}\\
C^{Vib}_{144} &= f^{(2,1)}G_1G_{1,1} + f^{(3)}G_{1,1,1}\\
C^{Vib}_{166} &= f^{(2,1)}G_1G_{1,1} + f^{(3)}G_{2,1}\\
C^{\boldsymbol{Vib}}_{\boldsymbol{456}} &= f^{(3)}G_{1,1,1}
\end{aligned} \tag{3}$$

where expressions for $f^{(n)}$ and G_n functions have taken as our previous paper [16].

The evaluation of bulk modulus (B), shear modulus (G), anisotropic ratio (A), Young's modulus (Y) and Poisson's ratio (σ) is achieved under this calculation. The stability criteria (Born criterion) for the crystalline materials of fcc crystal is given by:

$$\begin{aligned}
&B_V = B_R = (C_{11} + 2C_{12})/3 > 0;\\
&(C_{11} - C_{12})/3 > 0; \quad C_{44} > 0
\end{aligned} \tag{4}$$

where B_H or $B = (B_V + B_R)/2$, represent the bulk modulus correlated to elastic constants and subscripts V, H and R signifies Voigt, Hill and Reuss average technique [17].

Theoretical valuation of shear modulus (G) and bulk modulus (B) has been estimated following the approach [18]. According to Pugh, B/G defined as $G = (G_V + G_R)/2$, where $G_V = (C_{11} - C_{12} + 3C_{44})/5$ and $G_R = 5[(C_{11}-C_{12})\,C_{44}]/[4C_{44}+3(C_{11}-C_{12})]$. If the ratio B/G is less than 1.75, the material is brittle nature and if this ratio is greater than 1.75, then the material is ductile [19]. Cauchy pressure Cp [20] shows the nature of bonding in a material and given by $Cp = (C_{12} - C_{44})$. The value Cp is negative for brittle materials and positive for ductile materials. Elastic anisotropy (A) projected by Zener [21] is founded as $A = C_{44}/C_S$, which goes out to be the valuable condition for classifying compounds that are elastically anisotropic. The tetragonal shear modulus is $C_S = (C_{11} -$

C_{12})/2. The expressions for Young's modulus (Y) and Poisson's ratio (σ) is stated by:

$$Y = 9GB/(G+ 3B) \quad (5)$$

$$\sigma = (3B - 2G)/(6B + 2G) \quad (6)$$

For the characterization of nanomaterials, ultrasonic velocities have significant parameter. The ultrasonic wave propagation along <100>, <110> and <111> directions through the anisotropic materials will depend along the particular directions on the orientation of strains. We obtained three types of ultrasonic velocities one longitudinal (V_L) and two shears (V_{S1}, V_{S2}) [22].

Ultrasonic attenuation leading two processes, one is the phonon-phonon interaction (Akhieser type damping) and another one is thermoelastic loss at higher temperature. The formulations for calculation of the attenuation due to the phonon viscosity-mechanism for longitudinal and shear waves are given by Mason [23, 24]:

$$(\alpha/f^2)_{Akh.Long} = \frac{4\pi^2\tau_L E_o(D_L/3)}{2\rho V_L^3} \quad (7)$$

$$(\alpha/f^2)_{Akh.Shear} = \frac{4\pi^2\tau_S E_o(D_S/3)}{2\rho V_S^3} \quad (8)$$

Here, for longitudinal wave and shear wave, the acoustic coupling constants are D_L and D_S, E_o is the thermal energy density are given by:

$$D_L = 9 < (\gamma_i^j)^2 >_L - \frac{3<\gamma_i^j>_L^2 C_V T}{E_o} \quad (9)$$

$$D_S = 9 < (\gamma_i^j)^2 >_S \quad (10)$$

The expression for thermal relaxation time (τ) is given by:

$$\tau = \tau_S = \tau_L/2 = \frac{3K}{C_V V_D^2} \quad (11)$$

Using the Debye temperature (θ), thermal energy density (E_0) and specific heat per unit volume (C_V) can be evaluated [25], which is given as:

$$\theta = \frac{hV_D}{k}\left[\frac{3p}{4\pi}\frac{N_A\rho}{M}\right]^{1/3}, \quad (12)$$

here k, h, and N_A are the Boltzmann constant, Planck's constant and Avogadro number. p is the number of atoms. M and ρ are molecular weight and density of the material.

The expressions for Debye average velocity (V_D) [26] is given as:

$$V_D = \left(\frac{1}{3}\sum_{i=1}^{3}\int\frac{1}{V_i^3}\frac{d\Omega}{4\pi}\right)^{-1/3} \quad (13)$$

Thermo elastic loss is obtained by:

$$(\alpha/f^2)_{Th.} = \frac{4\pi^2<\gamma_i^j>^2 kT}{2\rho V_L^5} \quad (14)$$

Where ω is the angular frequency, k is the thermal conductivity of the nanomaterial. γ_i^j is the Grüneisen number, which is directly calculated using the nonlinear elastic constants (SOECs and TOECs)

II. Results and Discussion

The values of SOECs and TOECs are evaluated using the lattice parameter ($a = 2r_0$) 4.09Å and the hardness parameter (b = 0.4183Å) for the Ag NW [8]. The SOECs and TOECs are evaluated using Eqs. (2, 3) and are presented in Table 1.

There is total nine elastic constants evaluated (Table. 1), four (i.e., C_{11}, C_{44}, C_{144} and C_{166}) elastic constants are increasing and four (i.e., C_{12}, C_{111}, C_{112} and C_{123}) elastic constants are decreasing with the temperature, while elastic constant C_{456} are found to be constant for all the temperatures. The decrease or increase in stiffness constants is due to the decrease or increase in atomic interaction through temperatures. If the inter-atomic distance decrease or increases with temperature then interaction potential increases or decreases due to increase or decreases in stiffness constants. This type of properties has been previously found in other fcc-type materials [16, 22, 27, 28]. Elastic properties are significant because they corelate to the numerous essential solid-state phenomena like as equation of state, phonon spectra and inter-atomic potentials of silver nanowire. Comparing our results with the Debye temperature of silver nanowire. The current value of Debye temperature is 150.9 K, evaluated using SOECs, while the Debye temperature experimentally determined by Cheng et al. [8] is 151 K. Thus, there is good agreement between the present value and reported

Table 1

SOECs and TOECs [in GPa] of Ag nanowire at temperatures from 100 K - 300 K.

T [K]	C_{11}	C_{12}	C_{44}	C_{111}	C_{112}	C_{123}	C_{144}	C_{166}	C_{456}
100	68.2	66.2	66.8	-20.6	-252.3	88.7	89.9	-253.4	89.5
150	88.3	65.9	66.9	-15.7	-252.1	88.3	90.0	-253.7	89.5
200	122.1	65.8	67.0	-10.7	-251.8	87.8	90.2	-254.1	89.5
250	176.1	65.6	67.1	-9.2	-251.6	87.4	90.3	-254.4	89.5
300	230.4	65.4	67.2	-5.4	-251.3	87.0	90.5	-255.0	89.5

value by Cheng et al. Therefore, our theoretical calculations of higher order elastic constants to be justified for Ag NW. The chosen silver nanowire is mechanically stable, because the Born stability criterion as given in Eq. 4. Is satisfy.

Using Wiedemann-Franz law, the thermal conductivity (k) is evaluated by the consistent resistivity. The thermal energy density (E_0) and specific heat per unit volume (C_V) are evaluated using the Debye temperatures [25]. Temperature dependent 'k', density, thermal energy and specific heat per unit volume presented in Table (2).

The attained values of SOECs and TOECs are useful to calculate the bulk modulus (B), Young's modulus (Y), shear modulus (G), Cauchy pressure (C_P)**,** tetragonal moduli (C_S), Zener anisotropy factor (A), Poisson's ratio (σ) and B/G ratio. Temperature dependent values are presented in the Table 3 which shows that ratio B/G is less than 1.75 at above the temperature 200 K, which indicates that silver nanowire has brittle nature at these temperature range, while below than 200 K, it is ductile nature. Anisotropy factor is less than one only at room temperature for silver nanowire, so this has anisotropic behavior at room temperature, at other lower temperatures it's have greater than one, which plays a very significant role in manufacturing and material physics. The Cauchy pressure (C_P) discuss the bonding nature in the crystals and it have positive values, show to a more bonding ionic character in the materials and negative value shows directional bonding [29].

The ultrasonic velocities are vital parameters of the compounds to offer evidence about the crystallographic surface. Ultrasonic velocities (V_L and V_S) have evaluated using SOECs and density of the nanomaterials for longitudinal and shear modes of propagation along different crystallographic directions. Also, Debye average velocity (V_D) using ultrasonic velocities are evaluated from Eq. (13) and are shown in Tables 4 and 5. The ultrasonic velocity is increases with the increase temperature in all directions. It is clear from Table 5, the Debye average velocity is maximum along <100> direction for silver nanowire. Thus along <100> direction will be most suitable for wave propagation for the Ag NW.

The thermal relaxation time (τ) is the important ultrasonic parameter, which has the time required for the reestablishment of the thermal equilibrium distribution by the strain providing by the ultrasonic wave propagation in the crystals. A perusal of Table 5 reveals that the 'τ' decreases with temperature along all the crystallographic directions. Thermal relaxation time is found in picoseconds order for silver nanowire and shown in Table 5. It is obvious from Eq. (11) that thermal relaxation time is relative to the thermal conductivity (k), C_V^{-1} and V_D^{-2} and a perusal of Table (2) and (5) reveals that k, Cv and V_D increases with increase the temperature.

Table 2

Thermal Conductivity (k), density (ρ), specific heat (C_v) and thermal energy density (E_0) of Ag nanowire in the temperature range100 - 300 K.

T [K]	k x 10^2 (erg/sec. cm. K)	ρ (gm/cm^3)	C_V x 10^5 (erg/cm^{3}K)	E_0 x 10^7 (erg/cm^3)
100	100	0.865	17.97	10.88
150	135	0.845	17.99	19.79
200	163	0.825	18.34	28.46
250	180	0.805	18.96	36.99
300	200	0.785	18.66	44.93

Table 3

Young's modulus Y (in GPa), bulk modulus B (in GPa), shear modulus G (in GPa), Poisson's ratio σ, anisotropy factor A, fracture/toughness B/G and Cauchy pressure, C_P (in GPa) of Ag nanowire in the temperature range100 - 300 K.

T [K]	Y	G	B	A	C_P	σ	B/G
100	58.17	21.46	66.87	66.8	-0.6	0.36	3.12
150	87.22	33.5	73.37	5.97	-1	0.3	2.19
200	119.64	47.32	51.46	2.38	-1.2	0.26	1.09
250	103.31	62.09	102.43	1.21	-1.5	0.25	1.65
300	126.33	72.95	33.2	0.81	-1.8	0.13	0.46

Table 4

Ultrasonic velocity (10^3m/s) in Ag nanowire along different crystallographic directions in the temperature range100 – 300 K.

Direction	[100]		[110]			[111]	
T [K]	V_L	V_S	V_L	V_{S1}	V_{S2}	V_L	V_S
100	4.05	8.79	4.91	8.79	8.23	4.99	8.45
150	8.98	8.90	9.68	8.90	8.45	10.08	8.66
200	12.17	9.01	13.04	9.01	8.92	13.84	9.00
250	14.79	9.13	15.08	9.13	9.00	15.98	9.06

Table 5

Debye average velocity (V_D) and thermal relaxation time (τ) of Ag nanowire along different crystallographic directions in the temperature range100 - 300 K.

T [K]	V_D (10^3 m/sec)			τ (10^{-12}sec.)		
	[100]	[110]	[111]	[100]	[110]	[111]
100	5.77	5.11	4.92	5.00	5.05	5.12
150	12.79	12.09	11.73	1.32	1.37	1.43
200	17.31	16.92	16.24	0.88	0.95	1.05
250	21.01	20.80	20.00	0.67	0.72	0.84
300	24.28	23.02	22.01	0.57	0.63	0.79

Table 6

Average Grüneisen number $\langle\gamma_i^j\rangle_L$ for longitudinal wave, average square Grüneisen number $\langle(\gamma_i^j)^2\rangle_L$ and $\langle(\gamma_i^j)^2\rangle_S$ for longitudinal and shear wave of Ag nanowire along [100] direction from 100 K – 300 K.

T (K)	$\langle\gamma_i^j\rangle_L$	$\langle(\gamma_i^j)^2\rangle_L$	$\langle(\gamma_i^j)^2\rangle_S$
100	0.311	1.884	1.123
150	0.296	1.857	1.135
200	0.281	1.843	1.160
250	0.266	1.843	1.196
300	0.250	1.860	1.248

Table 7

Acoustic coupling constant for longitudinal (D_L) and shear (D_S) waves of Ag nano wire along different crystallographic directions in the temperature range100 - 300 K.

T [K]	D_L			D_S			
	[100]	[110]	[111]	[100]	[100]*	[110]**	[111]
100	16.482	44.20	37.948	0.627	10.103	5.43	14.744
150	16.356	46.41	36.073	0.613	10.219	5.76	15.133
200	16.282	49.23	34.357	0.601	10.436	6.144	15.647
250	16.123	52.82	32.895	0.591	10.656	6.579	16.31
300	16.102	57.34	31.692	0.582	11.227	7.088	17.154

**shear wave polarized along [001], **shear wave polarized along [1$\bar{1}$0]*

Temperature dependent average and square average ultrasonic Grüneisen parameter along different crystallographic directions of propagation are shown in Table 6 (evaluated using SOECs and TOECs). We have used average parameter, because these parameters taken a number of modes of propagation along different directions. Its p, which have significant role in study of anharmonic properties of nanowires. Also, it designates the physical properties of the nanowires such as thermal conductivity, thermal expansion and temperature discrepancy of elastic constants.

Along the different crystallographic directions, the temperature dependent acoustic coupling constant (D) have been calculated for Ag NW. We observe that D_L decreases along <100> and <111> directions and increases along <110> directions with temperature, while D_S is just about same along all the three directions (Table 7). The nature of D_L and D_S is similar to that of other fcc type compounds [30-32]. Therefore, the acoustic coupling constants (D_L, D_S) have not affected the temperature variation of the attenuation in the rang 100 - 300 K. Thus, elastic behaviour of the nanomaterials does not have important contribution to the total attenuation.

Along different crystallographic directions, the temperature dependent ultrasonic attenuation has been estimated for Ag NW using Eqs. 7, 8 and 14 under the condition $\omega\tau<<1$ and is shown in Figs. 1-3. The Akhieser loss of energy for longitudinal wave, shear waves and also thermoelastic loss increases with the temperature. Figs. 1-3 also designate that the ultrasonic attenuation due to thermoelastic relaxation and shear wave are smaller in comparison to the attenuation due to longitudinal wave. Thus, the main governing factor for this behaviour is the thermal conductivity and thermal energy density. It is very important to know the role of the microstructural phenomena, the allied physical properties and the related scientific parameters to the total ultrasonic attenuation at high temperatures.

The attenuation for thermal loss $(\alpha/f^2)_{th}$, is minimum at low temperatures and maxima for room temperature. Thermal loss corelated with the thermal conductivity (Eq. 14), which have dependent on Debye temperature (θ_D) and is minima and maxima as lower to higher temperatures. Shear loss is smaller in comparison to other types of losses; therefore, ultrasonic attenuation is affected due to phonon–phonon interaction in the silver nanowire.

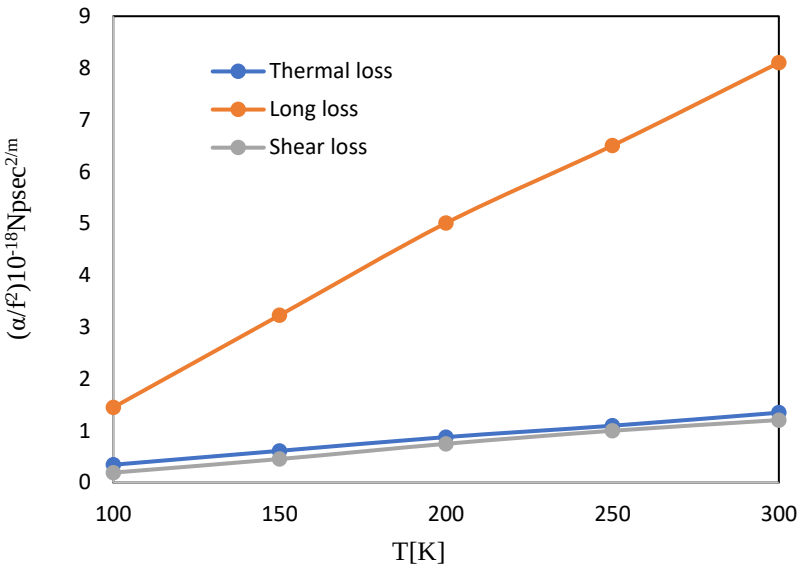

Fig. 1. Ultrasonic Attenuation $(\alpha/f^2)_{Th}$, $(\alpha/f^2)_{Akh.Long}$ and $(\alpha/f^2)_{Akh.Shear}$ along [100] direction in Ag nanowire..

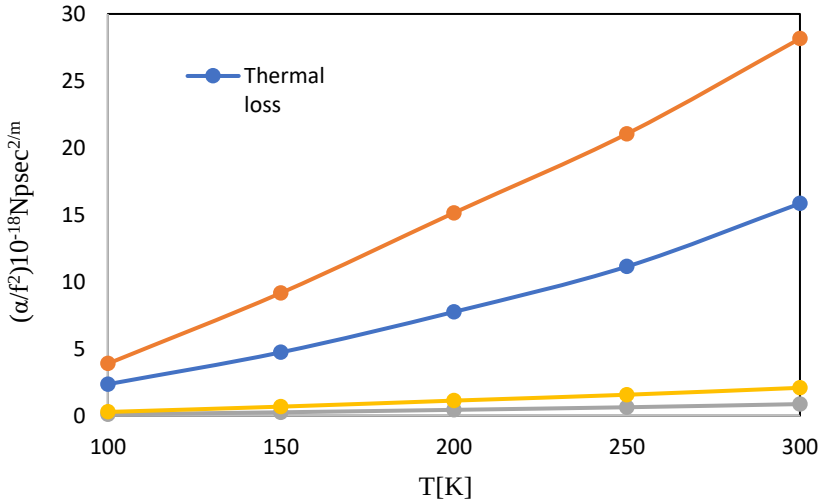

Fig. 2. Ultrasonic Attenuation $(\alpha/f^2)_{Th}$, $(\alpha/f^2)_{Akh.Long}$ and $(\alpha/f^2)_{Akh.Shear}$ along [110] direction in Ag nanowire. *shear wave polarized along [001] and **shear wave polarized along [1$\bar{1}$0].

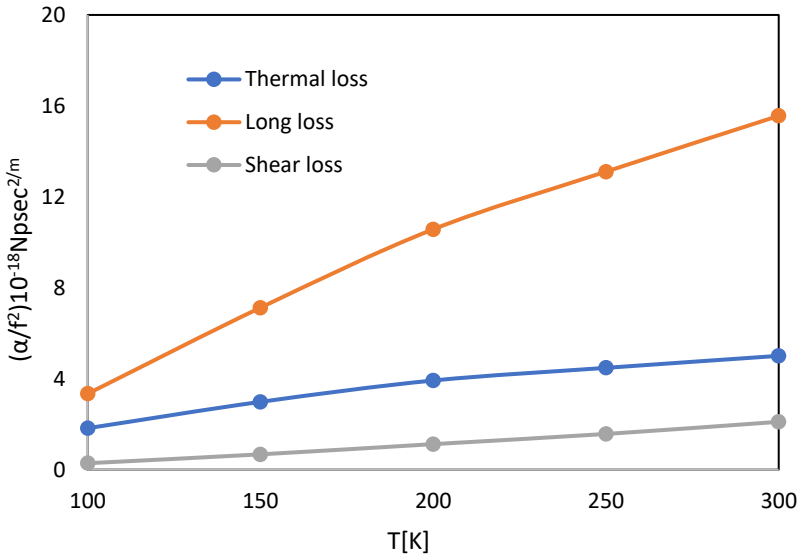

Fig. 3. Ultrasonic Attenuation $(\alpha/f^2)_{Th}$, $(\alpha/f^2)_{Akh.Long}$ and $(\alpha/f^2)_{Akh.Shear}$ along [111] direction in Ag nanowire.

Conclusions

Based on the above conversation is valuable to state that:

- Temperature dependent higher order elastic constants of the single crystal silver nanowire as well as their allied elastic properties, such as Young's modulus, bulk modulus, shear modulus and Poisson's ratio, are evaluated using the Coulomb and Born–Mayer potentials approaches.

- The mechanical characteristics of Ag NWs, like elastic anisotropy and ductile–brittle characteristic, are further estimated by evaluating the Cauchy pressures, fracture to toughness ratio, Zener anisotropy factor of this nanowire for the strength of nanowires.

- The study verifies that the silver nanowire is mechanically stable and have brittle nature and anisotropy on elasticity at room temperature.

- The order of thermal relaxation time for Ag NW is found to be order of picoseconds, due to their least relaxation time for silver nanowire, the minimum time for re-establishment of equilibrium for thermal phonon distribution exists.

- The acoustic coupling constant along longitudinal wave is greater than for shear waves.

- The ultrasonic attenuation increases with temperatures in all crystallographic directions, it has minimum at low temperature comparison to room temperature.

Study can be beneficial for the processing and non-destructive characterization [33] of silver nanowires. These results will provide a ground for investigating the major thermophysical properties in the field of other nanowires.

Yadawa P.K. - Ph. D., Associate Professor;
Chaurasiya N. - Ph. D., Assistant Professor;
Sachin Rai S. – Ph. D. Research Scholar;
Prajapati A.K. - Ph. D. Research Scholar.

[1] Z. Yu, L. Li, Q. Zhang, W. Hu, Q. Pei, Adv. Mater. 23, 453 (2011); https://doi.org/10.1002/adem.200300567.
[2] S. Kang, T. Kim, S. Cho, Y. Lee, A. Choe, B. Walker, S.- J. Ko, J. Y. Kim, H. Ko, Nano Lett. 15, 7933 (2015); https://doi.org/10.1021/acs.nanolett.5b03019.
[3] S. De, T. M. Higgins, P. E. Lyons, E.M. Doherty, P.N. Nirmalraj, W.J. Blau, J.J. Boland, J.N. Coleman, Acs. Nano. 3, 1767 (2009); https://doi.org/10.1021/nn900348c.
[4] L. B. Hu, H.S. Kim, J.Y. Lee, P. Peumans, Y. Cui, Acs. Nano. 4, 2955 (2010); https://doi.org/10.1021/nn1005232.
[5] L. Yang, T. Zhang, H. Zhou, S. C. Price, B. J. Wiley, W. You, ACS Appl. Mater. Interfaces. 3, 4075 (2011); https://doi.org/10.1021/am2009585.
[6] N. Stojanovic, J.M. Berg, D.H.S. Maithripala, M. Holtz, Appl. Phys. Lett. 95, 091905 (2009); https://doi.org/10.1021/am2009585.
[7] M. H. Chang , H.A. Cho, Y.S. Kim, E.J. Lee, J.Y. Kim, Nanoscale Res Lett. 9, 330 (2014); https://doi.org/10.1186/1556-276X-9-375.
[8] Z. Cheng, L. Liu, S. Xu, M. Lu, Z. Wang, Scientific Reports 5, 10718 (2015); https://doi.org/10.1038/srep10718.
[9] H. Gleiter, Acta Mater. 48, 1 (2000); https://doi.org/10.1016/S1359-6454(99)00285-2.
[10] S. Cuenot, C. Frétigny, S. Demoustier-Champagne, B. Nysten, Phys. Rev. 69, 165410 (2004); https://doi.org/10.1103/PhysRevB.69.165410.
[11] K. K. Caswell, C.M. Bender, C.J. Murphy, Nano Lett. 3, 667 (2003); https://doi.org/10.1007/s12598-010-0139-7.
[12] J. Y. Lee, S. T. Connor, Y. Cui, P. Peumans, Nano Lett. 8, 689 (2008); https://doi.org/10.1021/nl073296g.
[13] K. Brugger, Phys. Rev. 133, A1611 (1964); https://doi.org/10.1103/PhysRev.133.A1611.
[14] P. B. Ghate, Phys. Rev. 139, A1666 (1965); https://doi.org/10.1103/PhysRev.139.A1666.
[15] S. Mori, Y. Hiki, J. Phys. Soc. Jpn. 45, 1449 (1975); https://doi.org/10.1143/JPSJ.45.1449.
[16] P. K. Yadawa, R.R. Yadav, Multidiscipline Modeling in Materials and Structures 5, 59 (2009); https://doi.org/10.1108/15736105200900004.
[17] R. Hill, Proc. Phys. Soc., Sec. A 65, 349 (1952); https://doi.org/10.1088/0370-1298/65/5/307.
[18] D. Singh, S. Kaushik, S.Tripathi, V. Bhalla, A.K. Gupta, Arab J Sci Eng. 39, 485 (2014); https://doi.org/10.1007/s13369-013-0845-1.
[19] S. F. Pugh, Philos. Mag. 45, 823 (1954); https://doi.org/10.1080/14786440808520496.
[20] D. G. Pettifor, Mater. Sci. Technol. 8, 345 (1992); https://doi.org/10.1179/mst.1992.8.4.345.
[21] S. Bhajanker, V. Srivastava, G. Pagare, S.P. Sanyal, J. Phys.: Conf. Ser. 377, 01208037 (2012); https://link.springer.com/article/10.1007/s10765-016-2038-0.
[22] V. Bhalla, D. Singh, S.K. Jain, International Journal of Computational Materials Science and Engineering 5(3); 1650012 (2016); https://doi.org/10.1142/S2047684116500123.
[23] W. P. Mason, Academic Press Inc. 237 (1965); https://www.worldcat.org/title/physical-acoustics-principles-and-methods-vol-1-part-a/oclc/463203402.
[24] W. P. Mason, T.B. Bateman, J. Acoust. Soc. 40, 852 (1966); https://doi.org/10.1121/1.1910158.
[25] D. E. Gray ed., AIP Handbook, Mc Graw Hill Co. Inc. p.4-44, IIIrd edition. (New York, 1956); http://web.ipb.ac.id/~erizal/hidrolika/Chow%20-%20OPEN%20CHANNEL%20HYDRAULICS.pdf.
[26] C. Oligschleger, R.O. Jones, S.M. Reimann, H.R. Schober, Phys. Rev. 53(10), 6165 (1996); https://doi.org/10.1103/PhysRevB.102.099901.

[27] M. Landa, V. Novak, P. Sedlak, P. Sittner, Ultrasonics 42, 519 (2004); https://doi.org/10.1016/j.ultras.2004.01.029.
[28] D. Singh, D.K. Pandey, P.K. Yadawa, Cent. Eur. J. Phys. 7, 198 (2009); https://doi.org/10.1142/S0217984911027686.
[29] V. Kanchana, G. Vaitheeswaran, X. Zhang, Y. Ma, A. Svane, O. Erriksson, Phys. Rev. B 84, 205135 (2011); https://doi.org/10.1103/PhysRevB.84.205135.
[30] S.P. Singh, P.K. Yadawa, P.K. Dhawan, A.K. Verma, R.R. Yadav, Cryogenics. 100, 105 (2019); https://doi.org/10.1080/01411594.2020.1813290.
[31] P. K. Yadawa, Journal of Theoretical and Applied Physics 10, 203 (2016); https://doi.org/10.1007/s40094-016-0216-x.
[32] D. Singh, P.K. Yadawa, S.K. Sahu, Cryogenics 50, 476 (2010); https://doi.org/10.1016/j.cryogenics.2010.04.005.
[33] S. Mourdikoudis, R. M. Pallares, N. T. K. Thanh, Nanoscale 10, 12871 (2018). https://doi.org/10.1039/C8NR02278J.

П.К. Ядава, Н. Чаурасія, С. Рай, А.К. Праджапаті

Дослідження впливу температури на ультразвукові, механічні та теплові властивості нанодроту срібла

Кафедра фізики, Інститут фізичних наук професора Раджендра Сінгха (RajjuBhaiya) для вивчення та досліджень, Університет В. Б. С. Пурванчал, Джаунпур, Індія – 222003, pkyadawa@gmail.com
[2]Кафедра механічної інженерії, UNSIET, Університет В. Б. С. Пурванчал, Джаунпур, Індія – 222003

У роботі досліджено температурні залежності пружних, механічних та теплофізичних властивостей срібного нанодроту (Ag NW) на основі ультразвукових методів. Пружні константи вищого порядку розраховуються із використанням потенціалу Кулона та Борна-Майєра до другого найближчого сусіда. Для обчислення механічних параметрів, таких як модуль Юнга, модуль об'ємної пружності, тетрагональний модуль зсуву, коефіцієнт Пуассона, відношення руйнування до в'язкості та коефіцієнт анізотропії Зенера, із використанням пружних констант другого порядку, знайдено потрібні умови отримання срібного нанодроту з температурою. Нанодротини Ag при кімнатній температурі є крихкими. Оцінено ультразвукові швидкості, ультразвукові згасання через фонон-фононну взаємодію та термопружну релаксацію нанодротин срібла з використанням пружних констант вищого порядку для поздовжньої хвилі та зсувних хвиль уздовж кристалографічних напрямків <100>, <110> і <111> в діапазоні температур 100 - 300 K. Отримані результати обговорюються у порівнянні із існуючими результатами щодо таких властивостей нанодротин срібла.

Ключові слова: нанодротини срібла, пружні властивості, теплові властивості, ультразвукові властивості.